Article

# Enzymatic Synthesis of Layered Titanium Phosphates at Low Temperature and Neutral pH by Cell-Surface Display of Silicatein-

Paul Curnow, Paul H. Bessette, David Kisailus, Meredith M. Murr, Patrick S. Daugherty, and Daniel E. Morse

*J. Am. Chem. Soc.*, **2005**, 127 (45), 15749-15755• DOI: 10.1021/ja054307f • Publication Date (Web): 25 October 2005



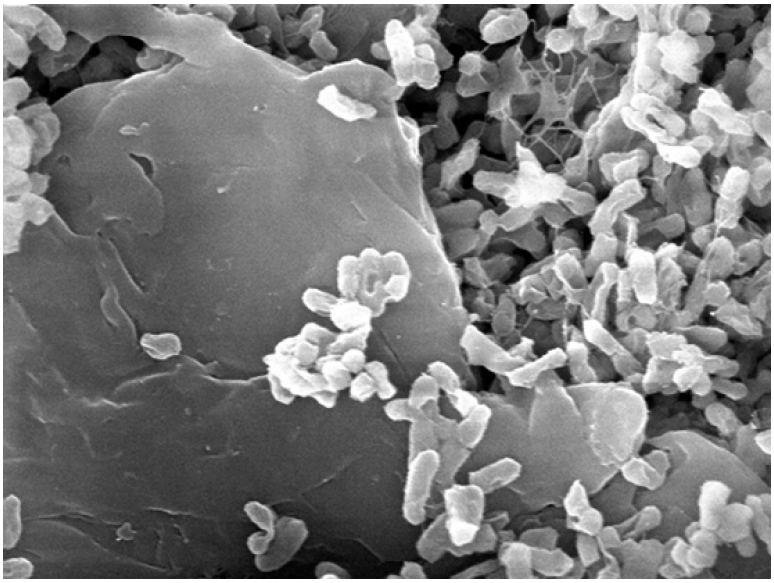

J|A|C|S
ARTICLES
Published on Web 10/25/2005

# Enzymatic Synthesis of Layered Titanium Phosphates at Low Temperature and Neutral pH by Cell-Surface Display of Silicatein-α

Paul Curnow,[†,‡,§] Paul H. Bessette,[∥] David Kisailus,[†,‡,§] Meredith M. Murr,[⊥] Patrick S. Daugherty,[†,‡,∥] and Daniel E. Morse*[,†,‡,§,⊥]

*Contribution from the Institute for Collaborative Biotechnologies, the California NanoSystems Institute, the Marine Biotechnology Center, the Department of Molecular, Cellular, and Developmental Biology, and the Department of Chemical Engineering, University of California at Santa Barbara, Santa Barbara, California 93106*

Received June 29, 2005; E-mail: d_morse@lifesci.ucsb.edu

***Abstract:*** We introduce a novel method of inorganic synthesis using the catalytic and structure-directing properties of the demosponge enzyme silicatein-α. Recombinant silicatein-α was displayed at the surface of *Escherichia coli* cells by fusion to outer membrane protein A and used to biocatalytically direct the formation of layered and amorphous titanium phosphates from a small water-soluble precursor at near-neutral pH at 16 °C. Synthesis of titanium phosphates, with potential applications in catalysis and separation technology, previously has required prolonged reactions with phosphoric acid at elevated temperatures. Additionally, we use library screening to isolate a 15-mer with affinity toward the silicatein active site ($K_d$ ca. 50 nM) and introduce this new approach to demonstrate the success of our display strategy. Considering our previous findings with native silicatein filaments, we suggest that this scalable, efficient, cell-based system may have a broad utility for the synthesis of a range of structured metallophosphates and other inorganic materials.

## Introduction

The formation of inorganic materials in biological systems proceeds at a physiological temperature and pH and generates structures with controlled nanoscale and microscale architectures that far exceed present anthropogenic capabilities.[1−3] As part of our efforts to take advantage of these processes for materials synthesis, we have previously isolated a group of enzymes from the filamentous protein aggregates occluded within the silica spicules of the pacific demosponge *Tethya aurantia*.[4] The major filament protein, termed silicatein-α, has a surprisingly high peptide sequence homology to the papainlike cysteine protease cathepsin L; one important distinction between the two is the substitution of serine for cysteine in the catalytic triad, considerably reducing the proteolytic activity of silicatein-α. Additionally, the unusual filamentous organization is significant because the orientation and chemical nature of silicatein surface residues is likely to play a key role in directing the in vivo growth characteristics of the demosponge spicules.

We have previously used *Tethya*-derived filament preparations to biocatalytically direct the synthesis of polymeric silica and polysilsesquioxanes from small silicon alkoxides in vitro.[5] Additionally, the wide synthetic utility of these filaments has been demonstrated in hydrolysis and polycondensation reactions at low temperatures (16−20 °C) and near-neutral pH to generate nanocrystalline/amorphous titanium dioxide from the precursor titanium(IV) bis(ammonium lactato) dihydroxide (Ti−BALDH)[6] and gallium oxo-hydroxide and spinel gallium oxide from gallium(III) nitrate.[7] In all cases, the templating capacity of the filament surface provides a degree of control over the nanoscale architecture of the inorganic product that cannot be achieved under alternative synthetic conditions.

One further development of this work will be the effective application of recombinant silicatein.[8] However, heterologous expression and reconstitution of the silicateins have proven difficult because of their high hydrophobicity, resulting in the formation of intracellular inclusion bodies of silicatein aggregates. Here, we present an alternative approach using a bacterial cell-surface display of recombinant silicatein-α to create a whole-cell biocatalyst for inorganic synthesis applica-

[†] Institute for Collaborative Biotechnologies.
[‡] California NanoSystems Institute.
[§] Marine Biotechnology Center.
[⊥] Department of Molecular, Cellular, and Developmental Biology.
[∥] Department of Chemical Engineering.

(1) Mann, S. *Nature* **1993**, *365*, 499−505.
(2) Heuer, A. H.; Fink, D. J.; Laraia, V. J.; Arias, J. L.; Calvert, P. D.; Kendall, K.; Messing, G. L.; Blackwell, J.; Rieke, P. C.; Thompson, D. H.; Wheeler, A. P.; Veis, A.; Caplan, A. I. *Science* **1992**, *255*, 1098−1105.
(3) van Bommel, K. J. C.; Friggeri, A.; Shinkai, S. *Angew. Chem., Int. Ed.* **2003**, *42*, 980−999.
(4) Shimizu, K.; Cha, J. N.; Stucky, G. D.; Morse, D. E. *Proc. Natl. Acad. Sci. U.S.A.* **1998**, *95*, 6234−6238.
(5) Cha, J. N.; Shimizu, K.; Zhou, Y.; Christiansen, S. C.; Chmelka, B. F.; Stucky, G. D.; Morse, D. E. *Proc. Natl. Acad. Sci. U.S.A.* **1999**, *96*, 361−365.
(6) Sumerel, J. L.; Yang, W.; Kisailus, D.; Weaver, J. C.; Choi, J. H.; Morse, D. E. *Chem. Mater.* **2003**, *15*, 4804−4809.
(7) Kisailus, D.; Choi, J. H.; Weaver, J. C.; Yang, W.; Morse, D. E. *Adv. Mater.* **2005**, *17*, 314−318.
(8) Zhou, Y.; Shimizu, K.; Cha, J. N.; Stucky, G. D.; Morse, D. E. *Angew. Chem., Int. Ed. Engl.* **1999**, *38*, 779−782.

tions. Successful expression of the fusion protein to $5 \times 10^4$ copies per cell and localization to the outer membrane were confirmed by gel-based analysis. A novel 15-mer with affinity for the silicatein active site (apparent $K_d = 53$ nM) was derived from screening of a cell-based peptide library and is used to demonstrate the surface presentation and nativelike folding of the recombinant silicatein-α. Upon incubation with the small inorganic precursor Ti−BALDH in phosphate-buffered saline (PBS), the catalytic and templating properties of the displayed enzyme result in the cell-surface deposition of a layered titanium phosphate with crystallographic *d* spacings of 8.297, 2.427, and 2.140 Å. This is accompanied by the accumulation of amorphous titanium phosphate in the periplasmic space, a process that is influenced by the presence of the surface product. This is the first use of a cell-surface display for the enzymatic synthesis of structured polymeric metal phosphates.

## Materials and Methods

**Molecular Biology.** The expression vector pB33OmpA containing *Escherichia coli* outer membrane protein A (OmpA) cDNA downstream of the arabinose-inducible $P_{BAD}$ promoter was previously engineered for cell-surface-display applications[9] by introducing two *SfiI* restriction sites at 4829 bp and 5216 bp, corresponding to regions immediately preceding extracellular loops 1 and 4 of OmpA. For our purposes, the latter site was removed through site-specific mutation using the Quikchange system (Stratagene). The silicatein-α insert was prepared by a polymerase chain reaction (PCR) performed on an existing clone[8] such that the gene was flanked by sequences corresponding to the remaining unique *SfiI* site. This insert was subjected to blunt-end ligation into pETBlue-1 (Novagen) before being excised with *SfiI* and cloned into the region corresponding to OmpA loop 1.

**Fusion Protein Expression.** Overexpression studies were performed in *E. coli* strain MC1061, and all cultures were grown in LB media supplemented with chloramphenicol at 25 μg/mL. Seed cultures (10 mL) were used to inoculate 500 mL of broth in a sterile 2.5 L flask, and these secondary cultures were grown at 37 °C with shaking at 250 rpm to A600 of 0.7−0.9. Fusion protein expression was induced by the addition of L-(+)-arabinose (Sigma) to a final concentration of 0.2% w/v, and cultures were grown for 6 h at either 37 or 25 °C. Cell viability was determined by the number of colony-forming units seen on agar plates after serial dilutions. Cells were harvested by centrifugation at 10000*g* for 15 min at 4 °C and stored at −80 °C.

**Sucrose Gradient Fractionation and Sodium Dodecyl Sulfate Polyacrylamide Gel Electrophoresis (SDS−PAGE).** When required, cell pellets were thawed and resuspended in 5 mL of 50 mM Tris, pH 7.4, 5% v/v glycerol, 50 mM NaCl, and 50 μL of a recombinant lysozyme (Novagen). After 30 min, cells were sonicated for 3 × 20 s before centrifugation at 16000*g* for 20 min at 4 °C. The pellet (inclusion body fraction) was resuspended in 10 mL of 1% SDS in 10 mM Tris, pH 7.4. The supernatant (soluble fraction) was centrifuged at 80000*g* for 1 h at 4 °C, and the resulting pellet (total cell membranes) was resuspended in 1 mL of 20% (w/v) sucrose in 10 mM Tris, pH 7.4. A 200 μL aliquot was removed and loaded onto a discontinuous sucrose gradient of 1 mL of 70% and 2 mL of 54% (w/v) sucrose in 10 mM Tris, pH 7.4, and centrifuged overnight at 80000*g* at 8 °C. Bands corresponding to inner membrane (20%/54% interface) and outer membrane (54%/70% interface) fractions were isolated and subjected to a 4-fold concentration using trichloroacetic acid precipitation.

For SDS−PAGE, all samples were mixed with an equivalent volume of 2× sample application buffer, heated to 80 °C for 10 min, and loaded onto a precast 4%−20% Tris−Gly SDS−PAGE gel (Invitrogen). Densitometric analysis was conducted using the NIH Image freeware (http://rsb.info.nih.gov/nih-image/).

**Generating a Novel Affinity Peptide Toward Silicatein-α.** Protocols for magnetic and fluorescence-activated cell sorting are detailed elsewhere.[9] Briefly, silicatein filaments were prepared from the spicules of the Pacific demosponge *Tethya aurantia* by demineralization in hydrofluoric acid.[5] For library screening, the pH of the final Tris extraction buffer was raised from 8.5 to 9.1 by cooling to 4 °C. After 30 min, this procedure formed dissociated silicatein oligomers at 0.5 mg/mL total protein concentration (M.M.M. and D.E.M., unpublished observations). This preparation was biotinylated using the Fluoreporter kit (Molecular Probes) according to the manufacturer's instructions, and the biotinylated oligomers were used to interrogate a cell-surface-displayed peptide library containing $5 \times 10^{10}$ individual 15-mer sequences cloned into the first extracellular loop of the *E. coli* outer membrane protein A and expressed as above. Successive rounds of screening by magnetic cell sorting (MACS) and fluorescence-activated cell sorting (FACS) resulted in $10^7$-fold enrichment in silicatein-binding sequences. The cDNA coding for seven of these recombinant peptides was obtained by miniprep (QIAgen) and sequenced.

**Binding to Surface-Displayed Proteins.** The peptide sequence demonstrating the highest affinity for the silicatein oligomers was synthesized at >95% purity by standard solid-phase chemistry (Sigma-Genosys) with a fluorescein label attached to the C-terminus at synthesis. Approximately $1 \times 10^7$ cells from two populations induced to express either the outer membrane protein A-silicatein-α (OmpA-Sil) fusion or a recombinant OmpA were incubated for 45 min on ice with the affinity peptide at concentrations between 0.1 and 200 nM. Cell-associated fluorescence was determined by FACS.

**Biocatalysis of Ti−BALDH Hydrolysis and Polycondensation.** Approximately $2 \times 10^9$ cells displaying OmpA-Sil were thawed from frozen stocks and washed once with autoclaved 1 × PBS (PBS; 8 g/L NaCl, 0.2 g/L KCl, 1.44 g/L $Na_2HPO_4$, 0.24 g/L $KH_2PO_4$, pH 7.4) before being incubated with 5% (w/w) Ti−BALDH (Aldrich) in 10 mL of PBS for 16−70 h at 16 °C with gentle mixing. When aggregate products were formed, these were isolated by settling under gravity. In control experiments, cells displaying OmpA-Sil were preincubated for 30 min with 0.1 mM phenylmethylsulfonyl fluoride (PMSF; Sigma) before introduction of Ti−BALDH.

**Microscopic and X-ray Analyses.** For microscopic and X-ray analyses, cell and aggregate samples were washed three times with 1 mL of MilliQ water before being resuspended in a small volume of the same, snap-frozen in liquid nitrogen, and lyophilized. For scanning electron microscopy (SEM), the lyophilysate was placed on glass cover slips with a plastic pipet tip and analyzed with a Vega TS 5130MM instrument (Tescan, Czech Republic). Representative micrographs were taken at random locations within the samples. For transmission electron microscopy (TEM), cells were dried onto holey-carbon copper grids (Ted Pella Inc., Redding, CA) before imaging at 200 kV (FEI T-20, Hillsboro, OR). Selected area electron diffraction (SAED) patterns of various regions were obtained.

**Powder X-ray Diffraction.** Powder diffraction measurements of lyophilized cell samples were taken with a Bruker D8 diffractometer. High-resolution diffraction ($2\theta-\theta$) spectra were obtained (0.0073°/step) between 23° and 28.5° $2\theta$. Thermal annealing was performed in 200° increments to 1000 °C via a thermocouple attachment. To allow full peak indexing, subsequent spectra were taken between 9° and 60° $2\theta$.

**Elemental Analysis.** Inductively coupled plasma atomic emission spectroscopy (ICP-AES) was performed on a Thermo Jarrell Ash instrument. Cells were incubated with Ti−BALDH as above, collected by low-speed centrifugation, and washed once with 50 mL of MilliQ water before being resuspended in 2 mL of the same, transferred to a preweighed 50 mL Falcon tube, and lyophilized overnight. The dry cell mass was determined, and the desiccant was solubilized in 20 mL of 18% HCl at 50 °C overnight. Remaining precipitates were removed

(9) Bessette, P. H.; Rice, J. J.; Daugherty, P. S. *Protein Eng., Des. Sel.* **2004**, *17*, 731−739.

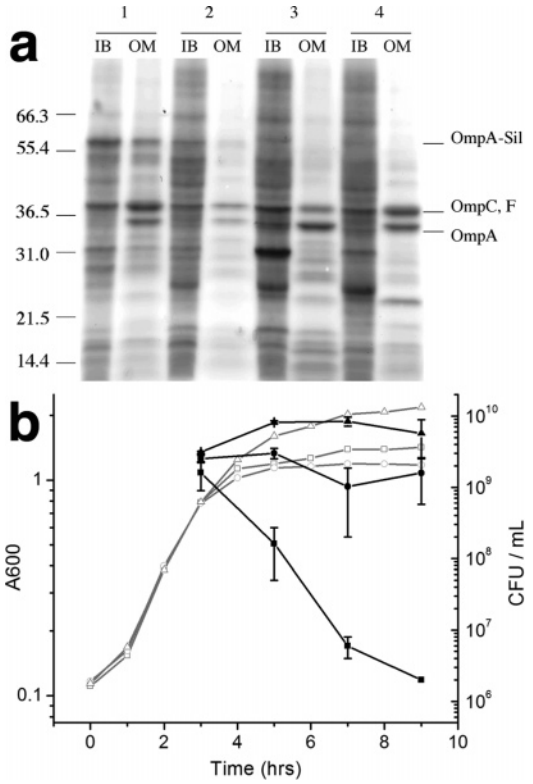


***Figure 1.*** Expression of the OmpA-Sil fusion protein. (a) SDS−PAGE of inclusion body (IB) and outer membrane (OM) cell fractions. Section 1: OmpA-Sil, 37 °C. Section 2: OmpA-Sil, 25 °C. Section 3: recombinant OmpA control, 37 °C. Section 4: uninduced control. Molecular weight standards are shown on the left in kDa. (b) Cell growth (open symbols) and cell viability (filled symbols). (□/■) Post-induction growth at 37 °C; (○/●) post-induction growth at 25 °C; (△/▲) uninduced control. Cultures were induced with 0.2% w/v L-arabinose at 3 h (A600 ca. 0.7). Error bars represent deviation from a mean average of two experiments.

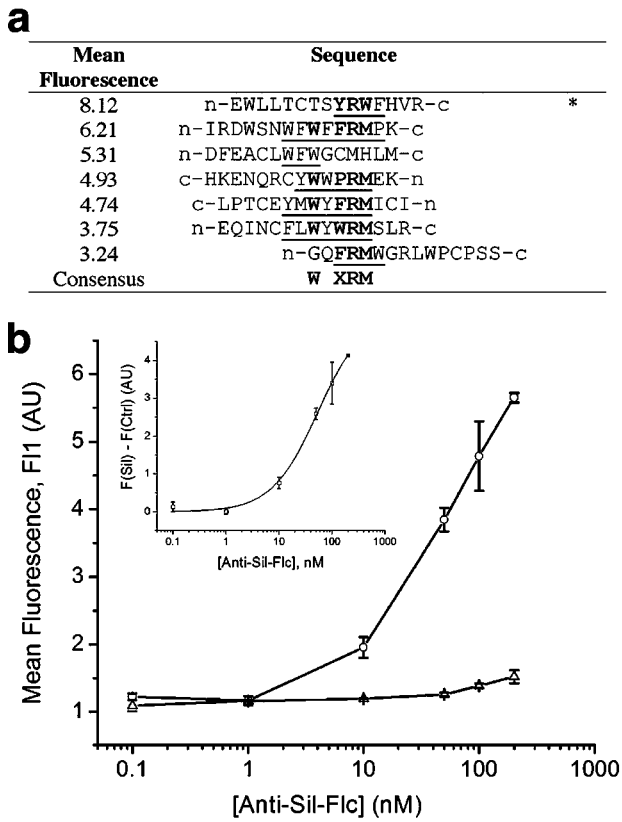


***Figure 2.*** Silicatein-binding peptides and their use in the characterization of displayed silicatein. (a) Peptide sequences isolated from library screening with silicatein filaments, arbitrarily aligned to show the conserved X−R−M binding motif. Sequence selected for further work denoted by *. (b) Binding of the fluorescein-labeled peptide (anti-Sil-Flc) to cells expressing OmpA-Sil (○) and recombinant OmpA (△). Error bars represent deviation from the average values from two experiments. Inset: fit of monovalent binding isotherm to background-corrected data by nonlinear regression.

by filtering through a 0.45 $\mu$m syringe-driven filter unit (Millipore), and this filtered solution was used directly in ICP after calibration with titanium and phosphorus standards (High Purity Standards, Charleston, SC). Readings were taken at several characteristic titanium and phosphorus lines, and signals at 323.4 and 185.9 nm, respectively, were compared between samples. The data were corrected for the dry cell mass, which was not seen to vary systematically.

## Results

**Fusion Protein Expression and Cell Viability.** The outer membrane protein A-silicatein-α (OmpA-Sil) fusion protein is localized exclusively within the inclusion body and outer membrane fractions of induced cells (Figure 1a) grown at 37 °C (section 1) and 25 °C (section 2). The apparent molecular weight of 58 000 Da is in good agreement with the predicted value of 60 373 Da (OmpA, 37 097 Da; silicatein-α, 23 276 Da). Densitometric analysis suggests that OmpA-Sil is present at approximately $5 \times 10^4$ copies per cell[10] and comprises 20−25% of the total OM protein. This correlates with previous work on the cell-surface expression of other recombinant proteins using this promoter system.[11]

A significant growth arrest was observed after postinduction growth at 37 °C (Figure 1b) with a concomitant decrease in cell viability (>99.8% of the original cell population rendered nonviable). The cell-like nonpropagating structures were indistinguishable from viable cells in cytometric and microscopic analyses and after incubation with a fluorogenic protease substrate, demonstrating that the integrity of the outer membrane was not compromised (not shown). Cultures grown at 25 °C postinduction retained levels of viability similar to those for the uninduced control (~100%). Expression of the recombinant OmpA control at 37 °C resulted in a similar growth arrest but had no effect on viability (not shown for clarity).

**Characterization of Displayed Silicatein-α Using a Novel Affinity Probe.** A cell-based library screening method, described in detail elsewhere,[9] was used to isolate novel peptide affinity probes toward silicatein-α (Figure 2a). Equilibrium binding studies using the highest-affinity peptide (Figure 2a, marked *) show a clear enhancement in binding to OmpA-Sil cells compared to that of the controls (Figure 2b). The background-subtracted data were fitted to a monovalent binding isotherm by nonlinear regression analysis (Figure 2b, inset), and an apparent $K_d$ of 53 ± 5.85 nM was derived ($\chi^2 = 0.0077$, $P = 0.99$). A similar FACS-based approach has previously been shown to provide reliable estimates of $K_d$ values.[12] In a subsequent experiment, this peptide was also found to bind to a recombinant nonfusion silicatein-α (kindly donated by M.

(10) Schweizer, M.; Schwarz, H.; Sonntag, I.; Henning, U. *Biochim. Biophys. Acta* **1976**, *448*, 474−491.
(11) Daugherty, P. S.; Olsen, M. J.; Iverson, B. L.; Georgiou, G. *Protein Eng.* **1999**, *12*, 613−621.
(12) Daugherty, P. S.; Chen, G.; Olsen, M. J.; Iverson, B. L.; Georgiou, G. *Protein Eng.* **1998**, *11*, 825−832.

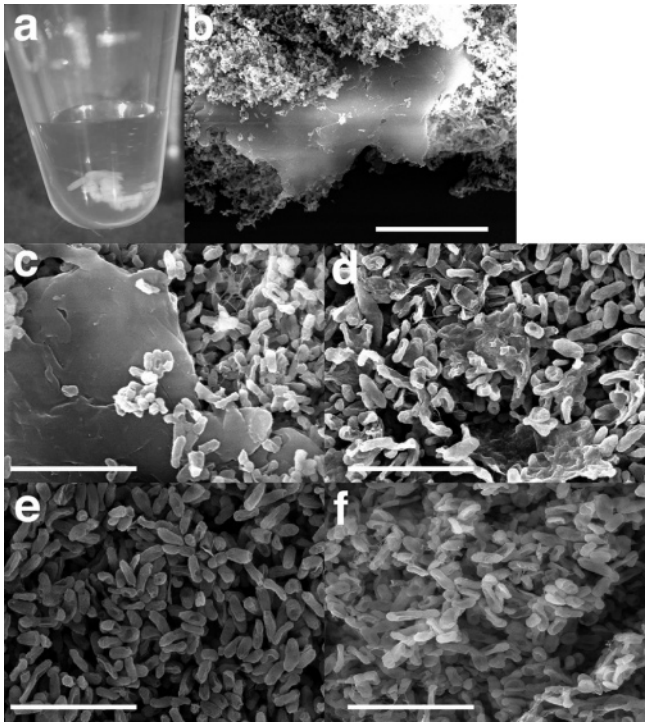


***Figure 3.*** Microscopic analysis of cells after reaction with Ti−BALDH. (a) Aggregates formed from cells expressing OmpA-Sil and (b) SEM of aggregates showing large sheet structures (scale bar of 20 $\mu$m). High-magnification SEM of (c) the aggregate products and (d) the remaining cell suspension shows increased cell-surface roughness and other morphologies not present (e) in control cells expressing recombinant OmpA and (f) in OmpA-Sil cells preincubated with PMSF (scale bar of 5 $\mu$m).

Izumi, UCSB) in a modified enzyme-linked immunosorbent assay (ELISA) procedure (not shown).

**Reaction of Cells with Ti−BALDH.** Silicatein-displaying cells formed large precipitates after reaction with the inorganic precursor Ti−BALDH (Figure 3a). Investigation by scanning electron microscopy (SEM) revealed smooth sheetlike structures over areas of >20 $\mu m^2$ uniquely in aggregate samples (Figure 3b; controls not shown). At higher magnifications, thin connective "threads" and sheetlike structures were seen in both aggregated (Figure 3c) and nonaggregated cells displaying OmpA-Sil (Figure 3d). These cell-surface products and morphologies are not present in control samples (Figure 3e,f).

We have not used the silicatein-binding peptide as a competitive inhibitor because the possibility that the peptide may be hydrolyzed by silicatein or endogenous proteases over the time course of our experiments would make any results ambiguous. Further characterization of this system, beyond the scope of the current work, would be required before such an experiment could be interpreted with confidence.

**Characterization of Bulk Reaction Products.** Powder X-ray diffraction on lyophilized cells (Figure 4) demonstrates that the bulk reaction products are amorphous at room temperature. Subsequent thermal annealing resulted in two crystalline phases. The first occurs at temperatures >600 °C and is characteristic of the rhombohedral sodium titanium phosphate $NaTi_2(PO_4)_3$ (JCPDS-ICCD # 33-1296) normally observed after heating the reaction products of $NaH_2PO_4 \cdot H_2O$, $(NH_4)_2HPO_4$, and anatase $TiO_2$.[13] The 100% intensity peak corresponding to a *d* spacing

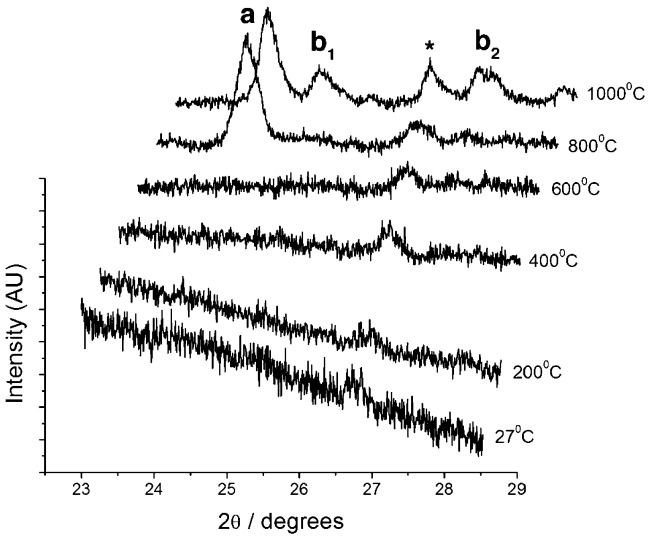


***Figure 4.*** Powder X-ray diffraction analysis of amorphous bulk reaction products before and after thermal annealing. (a) 100% intensity peak of rhombohedral sodium titanium phosphate, $NaTi_2(PO_4)_3$; $b_1$ and $b_2$ are characteristic strong lines of cubic $TiP_2O_7$. Instrument background peak denoted by *.

of 3.66 Å is shown here. The second phase, at temperatures >800 °C, corresponds to the cubic crystallite $TiP_2O_7$ (JCPDS-ICCD # 38-1468).[14] The 81% (marked $b_1$) and 72% (marked $b_2$) intensity peaks (3.52 and 3.22 Å, respectively) are shown. This compound has previously been formed by the reaction of anatase $TiO_2$ with 85% $H_3PO_4$ and subsequent heating to 1000 °C for several hours; other work also reports the transition of amorphous titanium phosphates to the cubic phase at 800−900 °C.[15] The figure is reduced for clarity, but scanning a wider angular range allowed full indexing of all peaks >15% relative intensity (not shown).

**Characterization of Cell-Surface Products.** Transmission electron microscopy (TEM) and selected area electron diffraction (SAED) reveal that the cell-surface products formed by OmpA-Sil are crystalline (Figure 5a). The diffraction pattern is characteristic of nanocrystalline products with *d* spacings of 8.297, 2.427, and 2.140 Å. A darkfield image taken in the spot plane (Figure 5b) clearly shows a crystalline phase at the cell surface. Control cells expressing a recombinant OmpA and OmpA-Sil cells after incubation with PMSF were not seen to have significant surface products (not shown).

**Influence of Surface Products on the Bulk Reaction.** Inductively coupled plasma atomic emission spectroscopy (ICP-AES) was used to quantify cell-associated titanium (Figure 6) and phosphorus (not shown). Cells expressing OmpA-Sil (Sil) accumulate ~1.5-fold less titanium than control cells that express a recombinant OmpA (OmpA) or are uninduced (Un). Additionally, the data show a nonintuitive trend in which cells expressing OmpA-Sil accumulate ~1.4-fold more titanium after preincubation with the protease inhibitor PMSF (Sil vs Sil+I). This is in direct contrast to both controls, in which introducing PMSF results in a ~1.4-fold decrease in the amount of titanium (OmpA+I, Un+I). A sample in which no Ti−BALDH was introduced is included for comparison (−Ti). Cell accumulation of phosphorus followed the same trend (not shown), and the

(13) *Natl. Bur. Stand., Monogr. (U.S.)* **1982**, *25*, 79.

(14) McMurdie, H. *Powder Diffr.* **1987**, *2*, 52.
(15) Costantino, U.; la Ginestra, A. *Thermochim. Acta* **1982**, *58*, 179−182.

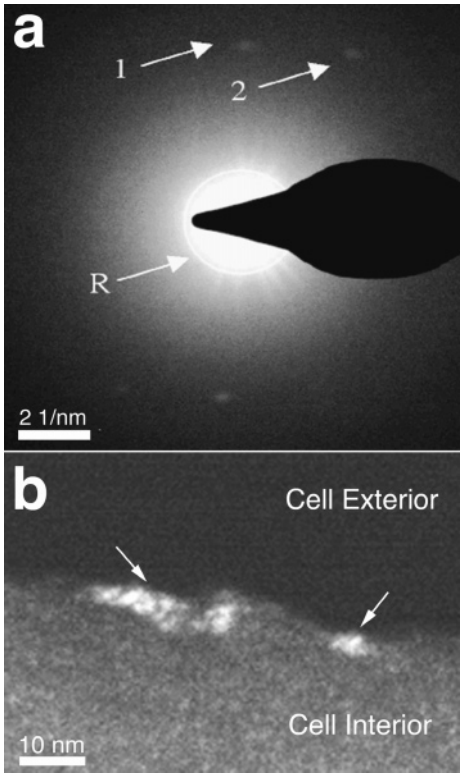


***Figure 5.*** TEM and SAED of cell-surface products. (a) Structures observed in the brightfield image are crystalline; the ring (R) is indicative of nanocrystallinity, and *d* spacings of the individual spots (arrows) are characteristic of layered titanium phosphates (see text). (b) Darkfield imaging further demonstrates the crystalline nature of the product (arrows).

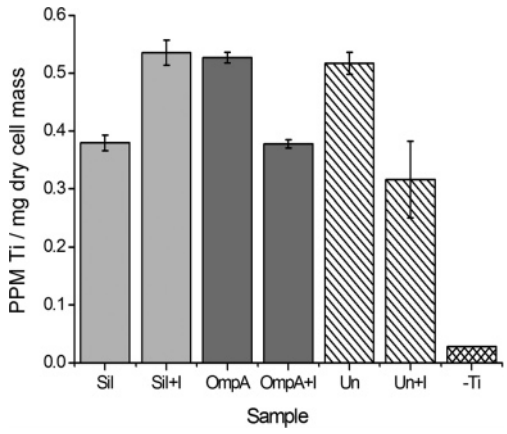


***Figure 6.*** Cell accumulation of titanium after incubation with Ti−BALDH, determined by ICP-AES. Cells expressing silicatein-α (Sil) or OmpA (OmpA) are compared to uninduced cells (Un) and equivalent reactions in which the protease inhibitor PMSF was introduced (+I). In the absence of Ti−BALDH, background levels of titanium are insignificant (−Ti). Error bars represent deviation from the mean average of two experiments. Individual data collection was highly reproducible (<1.5% RSD).

Ti/P ratio was 1:2.2−3.2 in all cases, consistent with the formation of bulk titanium phosphates. Additional wash steps, extended wash incubations, and longer reaction times had no effect on the data trends.

## Discussion

Bacterial cell-surface display of recombinant proteins and peptides has considerable potential as a biotechnological tool, with potential applications in whole cell enzymology,[16] vaccine development,[17] biosensors,[18] combinatorial library screening,[12] metal chelation,[19] and nanotechnology.[20] A range of different approaches have now been employed in pursuit of these goals, including recombinant fusion to endogenous outer membrane proteins.[21] "Sandwich" constructs, in which insertions are made into extracellular loops, have primarily been used to display unstructured peptides,[9,22] although the potential to accommodate large inserts has been appreciated.[23,24] Here, we describe for the first time the successful use of a sandwich-type fusion protein in the cell-surface display of an enzyme from a marine organism, silicatein-α, with novel catalytic and templating capabilities.

The OmpA-Sil construct is sorted to the outer membrane at high yields (Figure 1). Silicatein-α is highly hydrophobic, which may potentially be advantageous in a surface-display system by permitting translocation across the inner membrane. To enable additional characterization of the successful folding and/or presentation of the displayed protein, we screened a surface-displayed peptide library with native silicateins to identify silicatein-binding sequences (Figure 2a). A conserved motif of X−R−M was apparent in all but two of the peptide sequences, where X is an aromatic amino acid (W, Y, P, or F). Intriguingly, in the sequence that demonstrated the highest binding affinity, the otherwise conserved methionine residue is replaced by a tryptophan. We cannot distinguish whether this represents an actual increase in binding affinity, a higher expression level, or the ability to bind to the active site bidirectionally, increasing the relative fraction of the bound peptide. This sequence was selected for further work on the basis of binding affinity, high aqueous solubility, and lack of intrachain disulfides.

The high sequence similarity between silicatein-α and cathepsin L[4] suggests that they will have analogous tertiary structures. We therefore expect silicatein-α to have a small active site that recognizes substrates based primarily on main-chain and side-chain interactions at binding sites S2, S1, S1′, and S2′.[25,26] The S2 subsite is the only deep binding pocket and as such is the main determinant of substrate specificity; it accommodates bulky hydrophobic groups with optimal binding to phenylalanine. The S1 and S1′ subsites are binding surfaces that prefer positively charged residues and small hydrophobic groups, respectively.

We suggest that the repetitive selection of the X−R−M binding motif, and the high homology of this sequence compared to that of the known substrates for this family of enzymes, confers these peptides the ability to recognize the silicatein-α active site. On the basis of the discussion above, we predict that X binds at S2, R binds at S1, and M binds at S1′. Recent studies[27] have also suggested that tryptophan is particularly

(16) Francisco, J. A.; Earhart, C. F.; Georgiou, G. *Proc. Natl. Acad. Sci. U.S.A.* **1992**, *89*, 2713−2717.
(17) Lee, J.-S.; Shin, K.-S.; Pan, J.-G.; Kim, C.-J. *Nat. Biotechnol.* **2000**, *18*, 645−648.
(18) Mulchandani, A.; Kaneva, I.; Chen, W. *Anal. Chem.* **1998**, *70*, 5042−5046.
(19) Valls, M.; Atrian, S.; de Lorenzo, V.; Fernandez, L. A. *Nat. Biotechnol.* **2000**, *18*, 661−665.
(20) Sarikaya, M.; Tamerler, C.; Jen, A. K.-Y.; Schulten, K.; Baneyx, F. *Nat. Mater.* **2003**, *2*, 577−585.
(21) Lee, S. Y.; Choi, J. H.; Xu, Z. *Trends Biotechnol.* **2003**, *21*, 45−52.
(22) Freudl, R. *Gene* **1989**, *82*, 229−236.
(23) Sousa, C.; Kotrba, P.; Ruml, T.; Cebolla, A.; de Lorenzo, V. *J. Bacteriol.* **1998**, *180*, 2280−2284.
(24) Xu, Z.; Lee, S. Y. *Appl. Environ. Microbiol.* **1999**, *65*, 5142−5147.
(25) Barrett, A. J.; Rawlings, N. D.; Woessner, J. F. *Handbook of Proteolytic Enzymes*, 2nd ed.; Elsevier Academic Press: London, U.K., 2004; Vol. 2.
(26) Turk, D.; Turk, B.; Turk, V. In *Proteases and the Regulation of Biological Processes*; Saklatvala, J., Nagase, H., Salvesen, G., Eds.; Portland Press: London, U.K., 2003.

preferred at the S4 subsite, and it occurs at that position in four of the isolated sequences. Substrate binding by proteolytic enzymes is primarily determined by sequence specificity rather than structural recognition.[28] In simple energy minimization studies (J. J. Rice, P.C., and D.E.M., unpublished data), the peptides did not assume any higher-order structures.

Because the active site structure is only formed in folded, functional proteins, we predict that these peptides can be used as analytical tools to determine the physical state of recombinant forms of silicatein-α. The enhanced binding of one of these sequences to silicatein-displaying cells (Figure 2b) therefore suggests that a significant proportion of surface-displayed silicatein-α protrudes from the cell membrane in a nativelike state. We suggest that this approach could be readily applied to other displayed proteins and is potentially advantageous over current methods that detect unstructured epitope tags.[29]

Filamentous preparations of silicatein proteins have previously been shown to catalyze the formation of nanocrystalline/amorphous $TiO_2$ from Ti−BALDH in water.[6] From this and other studies on the silicateins,[5,7,8] we have proposed that the unusual active-site serine−histidine pair facilitates weak nucleophilic attack of inorganic substrates by the serine side-chain hydroxyl. This results in transitory Ser-O-substrate intermediates that are hydrolyzed to form reactive species that diffuse from the active site and condense with both other monomers and other oligomers of the inorganic precursors and with hydroxyl groups available on suitable surfaces. If these surfaces are patterned, as is the case with the organized silicatein filaments, the slow kinetics of the catalysis may permit the templated growth of metastable inorganic products. This can result in the formation of crystalline phases that are otherwise inaccessible under mild conditions.[6,7]

The results presented here indicate that this mechanism is replicated during materials synthesis with recombinant silicatein-α. However, during the enzymatic hydrolysis and subsequent polycondensation of Ti−BALDH, sodium and phosphate groups from the isotonic reaction buffer are incorporated into the titanium-based product (Figures 4−6). Attempts to reproduce these products through simple base catalysis (Ti−BALDH in PBS with varying concentrations of $NH_4OH$) generated titanium dioxide exclusively (not shown). The cell-catalyzed reaction therefore offers a unique approach to materials synthesis.

Using SAED, it is possible to focus on the diffractive properties of particular regions of the sample. We take advantage of this selectivity to exclusively analyze the crystalline nature of the surface products (Figure 5a). Additionally, the incident beam can be set in one of the observed diffraction planes, resulting in backscatter from regions that are crystalline within that plane (Figure 5b). Although precise structural characterization of the crystalline surface product is difficult from the weak diffraction pattern obtained here, the data are highly characteristic of the layered titanium phosphates, which have representative strong lines at 7−12 Å (corresponding to the interlayer distance).[30] The other *d* spacings are slightly below the values typically associated with these structures. Although we cannot rule out the formation of a novel structure because of the influence of cell-surface patterning, most likely a heterogeneous mixture of layered titanium phosphates is obtained with sodium incorporated at a certain number of sites. We are unable to perform a more detailed characterization of the surface products using the microscopic methods at our disposal. We also note that there is some ambiguity over the extent of sample heating under the TEM beam and that even slight increases in temperature can distort layered structures through partial dehydration and condensation.[31]

Layered metal phosphates are of commercial interest because they are efficient cationic exchangers and intercalators with high thermal and chemical stability (ref 30 and references therein). Cation-substituted forms have been used for hydrolysis, synthesis, polymerization, and redox chemistry,[32] and protonic conductance properties can be exploited in gas sensors[33] and photochemical reactions.[34] Additionally, organic functional groups can be introduced by simple chelation chemistry to generate supramolecular solid catalysts with a great number of potential applications.[30] Current synthetic strategies are primarily based on (a) refluxing, or thermal treatment, of amorphous titanium(IV) phosphates or anatase titanium dioxide with high concentrations (>5 M) of phosphoric acid;[31,35−38] (b) slow decomposition of titanium fluorocomplexes in phosphoric acid;[39] and (c) dissolution of titanium(III) salts in phosphoric acid to generate titanium(III) phosphates that are slowly oxidized in air to titanium(IV) phosphates.[40,41] Commonly, these reactions require high concentrations of phosphoric acid and incubation for several days at high temperatures (often >200 °C); mixed populations of the crystal phases are frequently obtained.

One intriguing aspect of our cell-based system is the bulk cellular accumulation of titanium phosphate and sodium titanium phosphate and the dependency of this on the activity of displayed silicatein-α (Figure 4 and Figure 6). Small hydrophilic molecules, such as Ti−BALDH (MW 294 Da), are able to diffuse from the cell exterior to the periplasmic space through porin channels.[42] Analogous to the putative mechanism of reaction with silicatein-α, Ti−BALDH is likely to be acted upon by any hydrolytic enzyme with a nucleophilic group within the active site. There is expected to be little, if any, specific binding requirement. We suggest that the high background observed in our experiments (Figure 6) is therefore a result of the nonspecific hydrolysis of Ti−BALDH by a wide range of endogenous periplasmic enzymes (i.e., those within the space between the outer cell wall and the cell membrane) and the consequent

(27) Portaro, F. C. V.; Santos, A. B. F.; Cezari, M. H. S.; Juliano, M. A.; Juliano, L.; Carmona, E. *Biochem. J.* **2000**, *347*, 123−129.
(28) Leung, D.; Abbenante, G.; Fairlie, D. P. *J. Med. Chem.* **2000**, *43*, 305−341.
(29) Becker, S.; Theile, S.; Heppeler, N.; Michalczyx, A.; Wentzel, A.; Wilhelm, S.; Jaeger, K.-E.; Kolmar, H. *FEBS Lett.* **2005**, *579*, 1177−1182.
(30) Alberti, G.; Clearfield, A.; Constantino, U. *Comprehensive Supramolecular Chemistry*; Pergamon-Elsevier Science: New York, 1996; Vol. 7.
(31) Krogh Andersen, A. M.; Norby, P. *Inorg. Chem.* **1998**, *37*, 4313−4320.
(32) Clearfield, A. *Inorganic Ion Exchange Materials*; CRC Press: Boca Raton, FL, 1982.
(33) Alberti, G.; Casciola, M. In *Proton Conductors*; Colomban, P., Ed.; Cambridge University Press: Cambridge, U.K., 1992; pp 238−253.
(34) Vliers, D. P.; Collin, D.; Schoonheydt, R. A.; De Schryver, F. C. *Langmuir* **1986**, *2*, 165−169.
(35) Alberti, G.; Cardini-Galli, P.; Constantino, U.; Torracca, E. *J. Inorg. Nucl. Chem.* **1967**, *29*, 571.
(36) Allulli, S.; Ferragina, C.; la Ginestra, A.; Massucci, M. A.; Tomassini, N. *J. Inorg. Nucl. Chem.* **1977**, *39*, 1043.
(37) Alberti, G.; Bernasconi, M. G.; Casciola, M.; Constantino, U. *J. Inorg. Nucl. Chem.* **1980**, *42*, 1637.
(38) Bruque, S.; Aranda, M. A. G.; Losilla, E. R.; Olivera-Pastor, P.; Maireles-Torres, P. *Inorg. Chem.* **1995**, *34*, 893−899.
(39) Alberti, G.; Constantino, U.; Giovagnotti, M. L. L. *J. Inorg. Nucl. Chem.* **1979**, *41*, 643.
(40) Tegehall, P.-E. *Acta Chem. Scand.* **1986**, *40*, 507.
(41) Bortun, A.; Jaimez, E.; Llavona, R.; Garcia, J. R.; Rodriguez, J. *Mater. Res. Bull.* **1995**, *30*, 413−420.
(42) Nikaido, H. *Microbiol. Mol. Biol. Rev.* **2003**, *67*, 593−656.

accumulation of hydrolysis products and Ti−BALDH within the periplasmic space. Because the periplasm constitutes ∼20−40% of the total cell volume,[43] the surface products formed at the exterior of OmpA-Sil cells (Figure 3c,d and Figure 5) represent a relatively small fraction of the bulk product.

We propose that the introduction of PMSF broadly inhibits these periplasmic enzymes, and less of the bulk product is formed in inhibitor-treated cells (Figure 6). However, in cells expressing OmpA-Sil, the enzymatic activity of silicatein-α generates cell-surface products that apparently *decrease* the transmembrane diffusion of Ti−BALDH into the periplasm, consequently reducing the bulk accumulation of polymerized products. Consistent with this suggestion, we see that PMSF inhibits silicatein-α function and so reduces the amount of polymeric product at the cell surface (Figure 3f). The surface-displayed protein also sequesters PMSF from solution, reducing the amount available to inhibit periplasmic enzymes; consequently, the bulk signal increases (Figure 6). The contrasting influence of PMSF observed in the different cell constructs makes it unlikely that the results arise from simple variations in cell physiology.

Considering the above, we hypothesize that the polymeric titanium phosphate products formed by silicatein-α at the cell surface are able to limit diffusion of Ti−BALDH across the outer membrane. We cannot differentiate whether this effect is the result of a solid diffusion barrier that occludes the porin channels or corresponds to a decrease in the external concentration as the precursor is consumed by reactions at the surface. However, given the large excess of Ti−BALDH and the relatively low amount of cell-surface product, we favor the former.

This experiment discloses three important features of the system. First, the presence of periplasmic enzymes is a key consideration when proteins of low catalytic activity such as silicatein-α are displayed; future studies may benefit from the use of protease-deficient bacterial strains.[44] Second, this issue is exacerbated when low-affinity, broad-range substrates such as Ti−BALDH that can diffuse across the outer membrane and are subject to hydrolysis by other catalytic moieties are used. Finally, microscopic examination is an important aspect of such experiments. Exploiting the structure-forming properties of OmpA-Sil in vitro, as opposed to the use of whole-cell assays, will therefore be a useful next step in further investigations of the system presented here.

(43) Neidhardt, F. C.; Ingraham, J. L.; Schaechter, M. *Physiology of the Bacterial Cell*; Sinauer Associates: Sunderland, MA, 1990.
(44) Meerman, H. J.; Georgiou, G. *Biotechnology* **1994**, *12*, 1107−1110.

## Conclusions

Biocatalytic routes to materials synthesis offer considerable advantages over current strategies. We present a novel approach in which a surface-displayed recombinant form of the enzyme silicatein-α is used to direct the synthesis of a layered titanium phosphate at the exterior of a bacterial cell. This is the first instance in which a recombinant silicatein has been used for ordered product formation, demonstrating that the filamentous organization of silicatein-α in vivo is not necessary for function in vitro. This also is the first report of an enzymatic route to titanium phosphate compounds. This scalable, rapid synthesis takes place at low temperatures and near-neutral pH, and we propose that this system will have broad utility for the synthesis of a range of metal phosphates, metal oxides, and other inorganic materials.

**Acknowledgment.** We thank G. Fu for suggesting the use of ICP and K. Roth for helpful discussions. This work was supported by grants from Oakridge National Laboratory (KC0206010), the U.S. Department of Energy (DE-FG03-02ER46006), the Institute for Collaborative Biotechnologies through grant DAAD19-03-D-0004 from the U.S. Army Research Office, NASA (University Research, Engineering, and Technology Institute on Bio-Inspired Materials (BIMat) under award No. NCC-1-02037 and NAG1-01-003), the NOAA National Sea Grant College Program, the U.S. Department of Commerce (NA36RG0537, Project R/MP-92) through the California Sea Grant College System, and the MRSEC Program of the National Science Foundation.

JA054307F